QUIJOTE MFI Data Release 1: Explanatory Supplement

QUIJOTE collaboration

v1.2: October 22nd, 2025

Contents

1 Introduction

This Explanatory Supplement is a reference text accompanying the public data products that result from the first QUIJOTE MFI wide survey Data Release

(DR1) [Rubiño-Martín et al., 2023]. It includes the description of all the products available via the QUIJOTE web pages[1] and the RADIOFOREGROUNDS project web pages [2].

MFI was a multi-channel instrument that operated between November 2012 and October 2018. It was mounted on the first QUIJOTE telescope. It consisted of four polarimeters (also called "horns"). Horns 1 and 3 operated in the band 10–14 GHz, while horns 2 and 4 operated at 16–20 GHz. Using frequency filters in the back-end module of the instrument, each horn provided outputs in two frequency sub-bands, each one with an approximate bandwidth of $\Delta\nu = 2$ GHz. There were a total of 8 outputs for each polarimeter, and these were then fed into the Data Acquisition Electronics. In total, the MFI provided four frequency bands centred around 11, 13, 17 and 19 GHz, with each band being covered by two independent horns.

The QUIJOTE MFI wide survey covers all the visible sky from the Teide Observatory (latitude 28.3°) with elevations greater than 30° (more than 29 000 deg^2). The final wide survey maps included in this release were obtained with approximately 9 000 h of observing time, and only use data from horns 2, 3 and 4.

The distribution of released data products associated with the QUIJOTE MFI wide survey papers contains the following items:

- Reduced Instrument Model containing basic parameters, beam radial profiles and window functions for each MFI horn, effective bandpasses and colour corrections (see Section 2).
- Final frequency maps (11, 13, 17, 19 GHz) in intensity and polarization, both at native and one degree resolution. Additionally, one set of null tests maps (half1/2 for independent baselines) (see Section 3).
- Radio source catalogues associated to the paper Herranz et al. [2023] (see Section 4).
- Maps obtained after component separation in polarization, as described in de la Hoz et al. [2023] (see Section 5.1).

2 QUIJOTE MFI: Instrument Model

The "Reduced Instrument Model" (hereafter RIMO) is a set of four FITS files containing selected characteristics of the QUIJOTE MFI instrument that are needed by users who work with the released data products.

The MFI wide survey contains 4 frequency maps, namely 11, 13, 17 and 19 GHz. Each frequency map is build from either one or two individual frequency maps per horn ("channels"). The maps at 11 and 13 GHz are directly those of horn 3, while the 17 and 19 GHz maps are obtained from the combination of two channels (from horns 2 and 4). To refer to individual channels (i.e., frequency

[1] QUIJOTE: `http://research.iac.es/proyecto/quijote`
[2] RADIOFOREGROUNDS: `http://www.radioforegrounds.eu/`

maps per horn), we follow the notation H =horn and FF=frequency, where H can be 2, 3 or 4, and FF takes values 11, 13, 17 and 19. The six channels used for the MFI wide survey are contributing to the final frequency maps as shown in Table 1.

Table 1: MFI channels contributing to the final maps.

Final map	MFI channels
11 GHz	311
13 GHz	313
17 GHz	217, 417
19 GHz	219, 419

The final maps at 17 and 19 GHz have been produced as a linear combination of those for horns 2 and 4. For simplicity in the computation of effective beams, frequencies and colour corrections, we adopted constant weights for this combination. Using these weights, that are given in Table 2, the combined map at 17 GHz is obtained as

$$m_{17} = w_{217} m_{217} + w_{417} m_{417}, \tag{1}$$

and similarly, the 19 GHz map is given by

$$m_{19} = w_{219} m_{219} + w_{419} m_{419}. \tag{2}$$

Note that the weight factors are different for intensity and polarization maps.

2.1 Basic parameters

The basic performance parameters describing the QUIJOTE MFI wide survey (horns contributing to each map, central frequencies, bandwidths and average beam properties) are summarised in Table 3. The electronic version of this table is given as a binary table in the file

`rimo_quijote_mfi_params_dr1.fits`

A detailed description of how all these parameters are computed is given in Génova-Santos et al. [2023].

Table 2: Constant weight factors used to produce the combined 17 and 19 GHz MFI wide survey maps. We include only the weight factors for horn 4, as those for horn 2 can be obtained as $w_{217} = 1 - w_{417}$ and $w_{219} = 1 - w_{419}$. Extracted from Table 9 in Rubiño-Martín et al. [2023].

	I	Q,U
w_{417}	0.362	0.732
w_{419}	0.419	0.788

Table 3: QUIJOTE-MFI basic performance parameters. Extracted from Table 3 in Rubiño-Martín et al. [2023].

Parameter	11 GHz	13 GHz	17 GHz	19 GHz
MFI horns contributing to these bands	3	3	2,4	2,4
Centre frequency (nominal), ν_0 (GHz)	11.1	12.9	16.8	18.8
Effective frequency[a] (GHz)	10.98	12.89	16.85	18.85
Bandwidth (GHz)	2.17	2.20	2.24	2.34
Beam FWHM (arcmin)	55.38	55.84	38.95	40.32
Main beam solid angle, $\Omega_{\rm mb}$ (10^{-4}sr)	2.748	2.781	1.362	1.428
Beam ellipticity[b], e	0.013	0.040	0.034	0.035
Antenna sensitivity, Γ (μK$_{\rm CMB}$/Jy)	961.9	703.8	847.0	645.2

[a] Computed for $\alpha = -1$, $\nu_e(\alpha = -1)$

[b] The ellipticity is defined here as $e = 1 - {\rm FWHM}_{\rm min}/{\rm FWHM}_{\rm max}$.

2.2 Beam radial profiles

The normalised (and radially averaged, 1D) beam radial profiles for all MFI channels contributing to the final wide survey maps are given in this FITS file:

`rimo_quijote_mfi_beamrp_dr1.fits`

The file contains a BINTABLE extension with the data. This extension consists of a 7-column table that contains the radial vector (θ, in degrees), and the six individual beam radial profiles, $r_{\rm p}^{HFF}(\theta)$ for each MFI channel. We follow the standard notation, with H =horn and FF=frequency. The six radial profiles are shown in the left panel of Figure 1.

The combination of maps from horns 2 and 4 is a linear process, and this linearity is preserved in the calculation of the "effective" beam. Therefore, the weighted mean of the radial profiles from horns 2 and 4, applying the coefficients shown in Table 2, would lead to the exact radial profiles of the effective beams corresponding to the combined maps at 17 and 19 GHz. For example, the radial profile for the 17 GHz map is given by

$$r_{\rm p}^{17\,{\rm GHz}}(\theta) = w_{217}\, r_{\rm p}^{217}(\theta) + w_{417}\, r_{\rm p}^{417}(\theta). \tag{3}$$

2.3 Beam transfer functions and window functions

The beam window functions for all MFI channels contributing to the final wide survey maps can be computed as

$$W_\ell = B_\ell^2, \tag{4}$$

where B_ℓ represents the corresponding beam transfer function. The beam transfer functions are given in this FITS file:

`rimo_quijote_mfi_beamtf_dr1.fits`

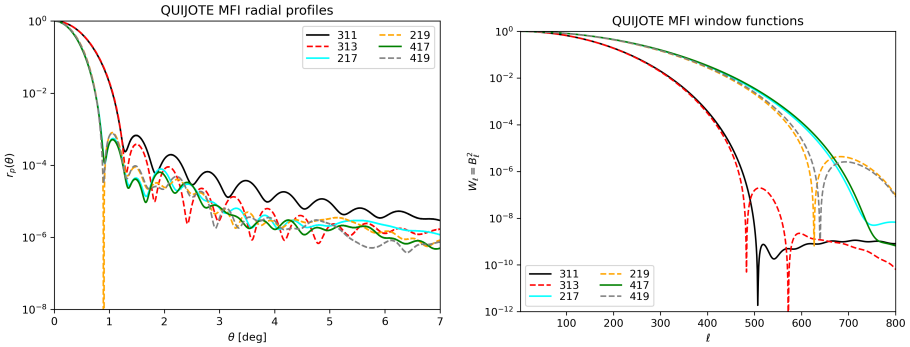

Figure 1: Left: Beam radial profiles. Right: Beam window functions.

The file contains a BINTABLE extension with the data. This extension consists of a 7-column table that contains the multipole (ℓ), and the individual beam transfer functions, B_ℓ^{HFF} for each MFI channel. We follow the usual notation H =horn and FF=frequency. The six window functions are shown in the right panel of Figure 1.

The calculation of the beam transfer function from the beam radial profile is a linear process. Therefore, as for the beam radial profiles (see previous section), linearity is also preserved in the calculation of the "effective" B_ℓ of the combined maps of horns 2 and 4. Then, the weighted mean of the B_ℓ of horns 2 and 4, using the coefficients shown in Table 2, would lead to the exact effective B_ℓ associated with the combined maps at 17 and 19 GHz. Effective window functions should be calculated by squaring these effective beam transfer functions. For example, the beam transfer function for the 17 GHz map is given by

$$B_\ell^{17\,\mathrm{GHz}} = w_{217}\, B_\ell^{217} + w_{417}\, B_\ell^{417}. \tag{5}$$

2.4 Effective band transmission profiles

The effective filter bandpasses for all MFI channels contributing to the final wide survey maps are given in

`rimo_quijote_mfi_bandpass_dr1.fits`

The file contains a BINTABLE extension with the data. This extension consists of a 9-column table. The frequency sampling of a given bandpass changes for different MFI horns. Thus, we provide a separated frequency vector for each horn. For horn 3, the frequency vector is given by FREQ_H3 (in GHz), and then two associated bandpass profiles for the 311 and 313 bands are given by BP_311 and BP_313, respectively. In summary, the 9 columns have names FREQ_H3, BP_311, BP_313, FREQ_H2, BP_217, BP_219, FREQ_H4, BP_417 and BP_419. The six bandpasses are shown in Figure 2.

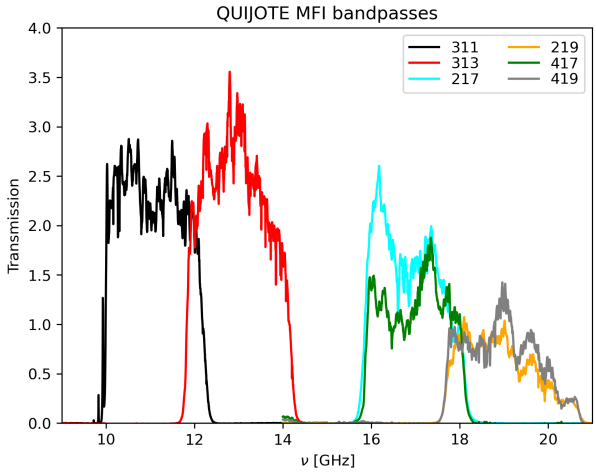

Figure 2: MFI effective band transmission profiles for horns 2, 3 and 4.

Bandpasses in QUIJOTE MFI are defined to provide the response in terms of the differential Rayleigh-Jeans brightness temperature ($T_{\rm RJ}(\nu)$), so the integrated voltage response of the system will be given by

$$V = G \int g(\nu) T_{\rm RJ}(\nu) d\nu, \tag{6}$$

where G is the overall gain. The bandpass profiles in the QUIJOTE RIMO file are given in unnormalized units. They can be normalized by forcing their integral to be equal to unity. For example, for horn 3, 11GHz, we would have

$$g_{311}(\nu) = \frac{BP_{311}(\nu)}{\int BP_{311}(\nu)\eta_{\Delta T}(\nu)d\nu}, \tag{7}$$

where $\eta_{\Delta T}(\nu)$ is the conversion factor from CMB temperature to RJ temperature. Similarly to the beam radial profiles and window functions, the effective bandpass of the combined maps of horns 2 and 4 can be obtained as the weighted mean of the two individual horns, using the coefficients from in Table 2. For example, the normalized bandpass for the 17 GHz map is given by

$$g_{17\,\rm GHz}(\nu) = w_{217}\, g_{217}(\nu) + w_{417}\, g_{417}(\nu), \tag{8}$$

where $g_{217}(\nu)$ and $g_{417}(\nu)$ are the normalized bandpasses for 217 and 417, respectively.

2.5 Colour corrections

The colour corrections for the MFI wide survey maps can be derived from the associated bandpasses given in the previous subsection, following the procedures explained in Génova-Santos et al. [2023].

Table 4: Colour correction coefficients, $C(\alpha, \nu_0) = c_0 + c_1\alpha + c_2\alpha^2$. The colour corrected temperature is obtained as $C(\alpha, \nu_0)T$, with T being the uncorrected measurement. Extracted from Table 4 in Rubiño-Martín et al. [2023].

Band	ν_0	c_0	c_1	c_2
11	11.1	0.981	0.0125	-0.0015
13	12.9	1.001	0.0018	-0.0012
17	16.8	1.007	-0.0022	-0.0007
19	18.8	1.007	-0.0020	-0.0008

Once they have been computed, colour corrections can be accurately described in terms of second order polynomials as a function of the spectral index α. For a sky emission having a flux density law $S_\nu \propto \nu^\alpha$, the coefficients $C(\nu_0, \alpha)$ provide the multiplicative correction factor to the measured flux density for the MFI frequency map at nominal frequency ν_0. These corrections are almost identical for intensity and polarization. Table 4 contains the coefficients for the final MFI wide survey maps. These numbers are also included in the public code FASTCC [Peel et al., 2022].

In order to reproduce the numbers above, we note that calculation of the exact colour corrections to be applied to the combined maps at 17 and 19 GHz entails calculation of the colour corrections of horns 2 and 4 independently. Then the final coefficient for a given frequency $FF = 17$ or 19 GHz, should be calculated as

$$C_{FF} = \frac{1}{\frac{w_{2FF}}{C_{2FF}} + \frac{w_{4FF}}{C_{4FF}}} \quad , \tag{9}$$

where $w_{2FF} = 1 - w_{4FF}$ and w_{4FF} is the weight quoted in Table 2 for frequency FF. This combination is also included in FASTCC and can be called directly.

3 QUIJOTE MFI DR1: maps

This section presents the QUIJOTE MFI wide survey maps described in Rubiño-Martín et al. [2023]. They correspond to four maps at nominal frequencies 11, 13, 17 and 19 GHz. As explained above, the maps at 11 and 13 GHz are directly those obtained from MFI horn 3. However, the maps at 17 and 19 GHz have been produced as a linear combination of those for MFI horns 2 and 4, using the constant weights given in Table 2. All QUIJOTE MFI sky maps and associated masks are presented in HEALPix format with RING ordering, with a default value of $N_{\rm side} = 512$, and using Galactic coordinates. Sky maps contain Stokes I, Q and U parameters, which are given in CMB thermodynamic units ($\mathrm{mK_{CMB}}$). Stokes Q and U parameter maps follow the COSMO convention[3] for polarization angles from HEALPix. In order to convert from COSMO to IAU, you have to swap the sign of the U Stokes parameter.

[3] `https://healpix.jpl.nasa.gov/html/intronode12.htm`.

The global properties of these MFI wide survey maps (noise levels in intensity and polarization, correlation properties between different maps, atmospheric residuals, etc) are described in Rubiño-Martín et al. [2023]. As a summary, we mention here that the sensitivities in polarization (Stokes Q and U maps) are within the range 35–40 μK per 1-degree beam. In intensity, they are within the range 60–200 μK per 1-degree beam (due to the MFI receiver design, the $1/f$ component is not cancelled by the correlation receiver in the intensity measurements; for this reason, the intensity maps have clear $1/f$ residuals on large scales, particularly in the two highest frequency bands). Moreover, there are also well-known noise correlations at the TOD level (also called "common mode $1/f$ noise") between channels of the same horn, which are inherited by the final maps. Because of this, the 11 and 13 GHz maps have some common (correlated) noise, and the same happens with the 17 and 19 GHz maps.

3.1 FDEC filtering

After the map-making step, the resulting MFI maps still present some residual RFI and large-scale patterns, which are corrected during a post-processing stage. As explained in Rubiño-Martín et al. [2023], generally the residual RFI signals appear at fixed azimuth locations, and thus these features are projected onto the maps in stripes of constant declination.

This residual RFI is removed using a function of the declination (hereafter FDEC), which is extracted directly from the maps as the median of all pixels with the same declination. This template function is built using a $|b| < 10^\circ$ mask to exclude emission from the Galactic plane, and specific masks in intensity and polarization for each frequency channel excluding the 10 per cent of the brightest pixels. The procedure is applied, separately, both in intensity and polarization. In polarization, the maps are first rotated to local (equatorial) coordinates in order to extract the correction function. In this way, the RFI contamination from static sources in local coordinates appears as a constant signal in a given declination band. The code for performing this FDEC filtering can be obtained from `https://github.com/jarubinomartin/sancho` (IDL and Python versions available).

When correlating the final QUIJOTE MFI wide-survey maps with external datasets, it should be taken into account that those large scale modes are not present in the QUIJOTE maps. For a direct comparison, the FDEC filtering should also be applied to the external datasets.

3.2 Masks

In this data release we include two specific sky masks related to QUIJOTE MFI analyses.

```
mask_quijote_ncp_lowdec_satband_nside512.fits
mask_quijote_satband_ncp86_nside512.fits
```

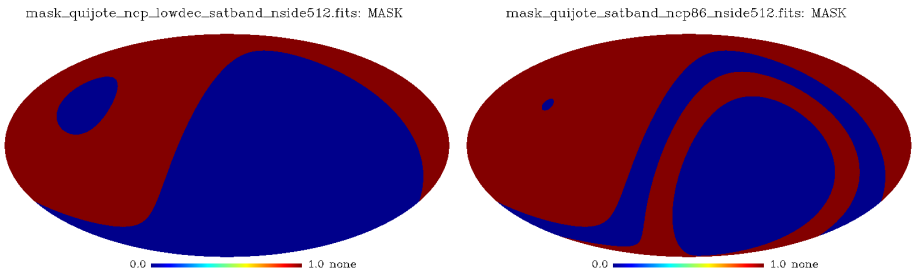

Figure 3: Masks associated to the QUIJOTE DR1. Left: standard analysis mask (NCP+lowdec+satband). Right: satband+npc86.

The first one corresponds to the default analysis mask used for most of the scientific analyses in the QUIJOTE MFI papers. It excludes the North Celestial Pole region for declinations above $\delta = 70°$, the low declination region below $\delta = -12°$, and the satellite band ($-12° < \delta < 6°$). The second mask, labelled as satband+ncp86, is applied by default to all the released MFI maps to exclude emission in the geostationary satellite band, and to keep the same sky coverage around the NCP in all maps (removing declinations above $\delta = 86°$). Both masks are depicted in Figure 3.

3.3 Frequency maps at original resolution

The main version of the frequency maps correspond to the MFI wide survey maps at their native (original) angular resolution. The FITS filenames are of the form:

`quijote_mfi_skymap_XXghz_NSIDE_dr1{coverage}.fits`

where XX are two digits to indicate the nominal QUIJOTE MFI frequency band (possible values are 11, 13, 17 and 19), "NSIDE" is the HEALPix $N_{\rm side}$ value of the map (default is 512), and "coverage" indicates which part of the database is used in each map (for this data release, no tag indicates full data, but we also provide also half mission nulltest maps named half1 and half2). For the full dataset, we present four maps:

`quijote_mfi_skymap_11ghz_512_dr1.fits`

`quijote_mfi_skymap_13ghz_512_dr1.fits`

`quijote_mfi_skymap_17ghz_512_dr1.fits`

`quijote_mfi_skymap_19ghz_512_dr1.fits`

The file sizes are approximately 108MB each.

The FITS files for these sky maps contain a minimal primary header with no data, and a BINTABLE extension containing the data. This extension consists

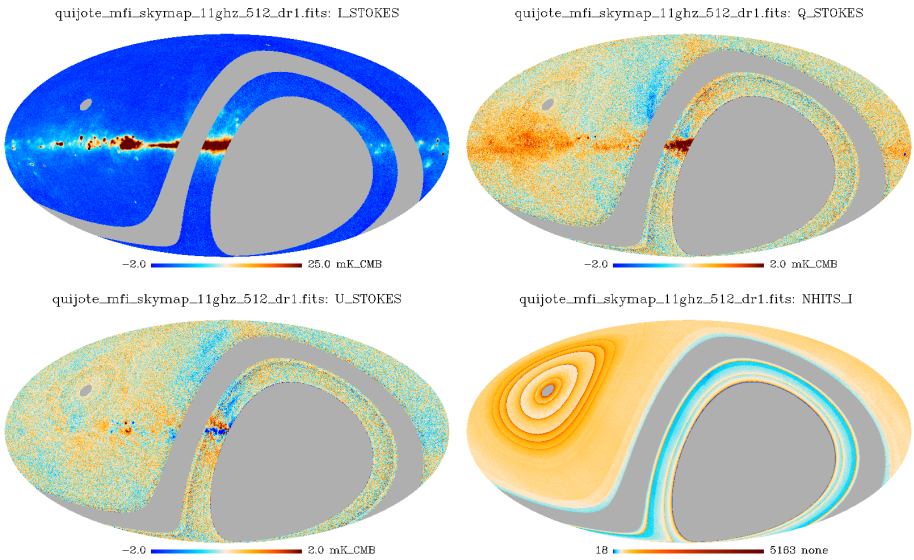

Figure 4: The first four columns of the MFI 11 GHz FITS file, showing I, Q, U, and NHITS_I respectively.

of a 9-column table that contains the signal (Stokes I, Q and U parameters), hit-counts for intensity and polarization maps (same for Q and U), weight maps for I, Q and U, and the covariance between Q and U, all in HEALPix format (see details in Table 5 below). Checksum values are included in the extended headers. Hit counts correspond to the number of 40 ms samples contributing to each pixel. We recall that the original MFI data sampling rate was 1 ms, but for the generation of the wide survey maps, all time streams are binned in 40 ms samples. Thus, the total integration time per pixel in seconds can be obtained as $0.04 N_{\rm hits}$.

The binning process allows us to assign a variance σ_i^2 to each binned sample i, which we used to define the associated weights ($w_i = 1/\sigma_i^2$). When propagated through the entire pipeline and map-making steps, the resulting weight maps are generated. They are delivered here, together with the associated covariance maps between Stokes Q and U parameters. Both the weight and covariance maps are renormalised using the factors described in Table 12 of Rubiño-Martín et al. [2023] to also account for residual 1/f noise. In this way, we guarantee that they properly match the one-point statistics for noise levels derived from the nulltest maps.

Keywords in the extended header indicate the coordinate system ("GALACTIC"), the HEALPix ordering scheme ("RING"), the telescope name ("QUIJOTE QT1"), the list of MFI channel(s) used, and central frequency ("FREQ"). The "COSMO" polarization convention is specified in the "POLCCONV" keyword. The "COMMENT" fields provide a basic summary of the product, and

Column name	Data type	Units	Description
I_STOKES	Real*4	$\mathrm{mK_{CMB}}$	Stokes I map
Q_STOKES	Real*4	$\mathrm{mK_{CMB}}$	Stokes Q map
U_STOKES	Real*4	$\mathrm{mK_{CMB}}$	Stokes U map
NHITS_I	Real*4	none	hits in I map
NHITS_QU	Real*4	none	hits in Q and U map
WEI_I	Real*4	$(\mathrm{mK_{CMB}})^{-2}$	Weight of I map
WEI_Q	Real*4	$(\mathrm{mK_{CMB}})^{-2}$	Weight of Q map
WEI_U	Real*4	$(\mathrm{mK_{CMB}})^{-2}$	Weight of U map
COV_QU	Real*4	$(\mathrm{mK_{CMB}})^{2}$	Covariance Q-U map

Table 5: QUIJOTE MFI sky map file data structure.

the "HISTORY" field contains the internal reference name of the final map used for this data release.

The "BAD_DATA" keyword gives the value used by HEALPix to indicate pixels for which no signal is present (unobserved pixels, or in the case of polarization maps, those with condition number out of range, as explained in Rubiño-Martín et al. [2023]).

3.4 Frequency maps at 1 degree resolution

For the maps smoothed to 1 degree resolution, the FITS filenames use the same convention as those maps at original resolution, but we insert in the name the text "smth". So for example,

```
quijote_mfi_smth_skymap_11ghz_512_dr1.fits
```

is the QUIJOTE MFI sky map at 11GHz and smoothed to 1 degree resolution.

Smoothed maps at 1° resolution are generated by convolving the original maps with the corresponding transfer function $T_\ell \equiv B_\ell^{1\,\mathrm{deg}}/B_\ell^{\mathrm{MFI}}$, which converts the spherical harmonic transfer function for each horn (B_ℓ^{MFI}, see Sect. 2.3) into that of a Gaussian beam with FWHM= 1° ($B_\ell^{1\,\mathrm{deg}}$). Figure 5 shows one example of the released smoothed maps.

4 QUIJOTE MFI DR1: catalogues

In this release we include two separate catalogues of point sources. The elaboration of the catalogues is described in Herranz et al. [2023]. The positions in the sky of the sources in the joint MFI DR1 catalogues is plotted in Figure 6. The first of the two catalogue FITS files corresponds to the MFI DR1 main sample (`quijote_mfi_psc_main_dr1.fits`), containing 47 targets. The second file corresponds to the extended sample (`quijote_mfi_psc_extended_dr1.fits`), containing 739 targets. Here we summarize the catalogue contents:

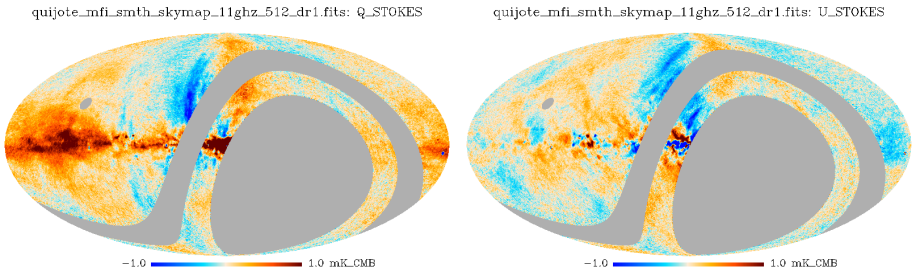

Figure 5: Second and third columns of the smoothed MFI 11 GHz FITS file, corresponding to Q and U.

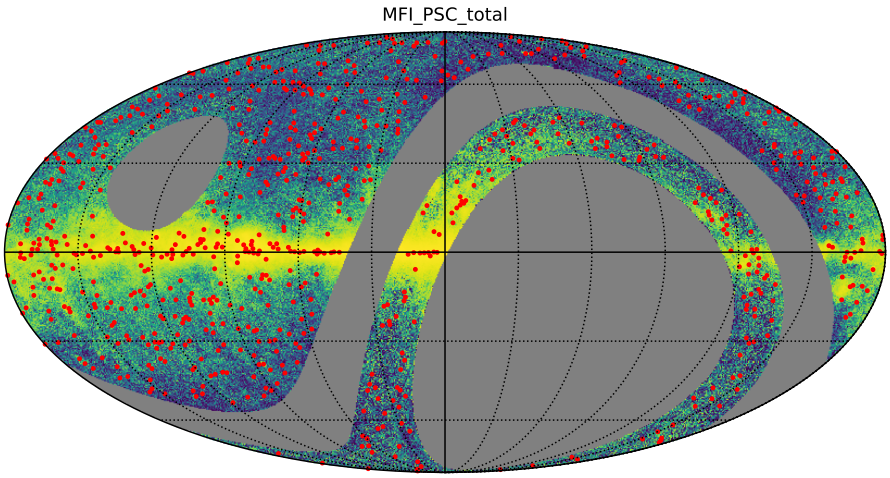

Figure 6: Position in the sky of the sources from the MFI DR1 point source catalogues.

– Source identification: a numeric identificator containing the string `'MFI-PSCm'` for the case of the main sample and `'MFI-PSCe'` for the case of the extended sample.

– Position: GLON and GLAT contain the Galactic coordinates; RA and DEC give the same information in equatorial coordinates (J2000).

– Stokes parameters: I, Q and U in Jy, and their associated uncertainties, for the four MFI frequencies (11, 13, 17 and 19 GHz). Values are not colour-corrected. Colour-corrections can be obtained using the public `fastcc` code (see Section 2.5).

– Polarization: debiased P and its associated uncertainty, in Jy, for the four MFI frequencies (11, 13, 17 and 19 GHz). Values are calculated from the raw (non colour-corrected) Stokes parameters.

– Polarization fraction and its associated uncertainty for the four MFI frequencies, as calculated from I and debiased P.

– Polarization angle: ϕ and its associated uncertainty, in degrees, for the four MFI frequencies (11, 13, 17 and 19 GHz). The polarization angles are defined as increasing anticlockwise (north through east) following the IAU convention; the position angle zero is the direction of the north Galactic pole.

– Statistical significance of the detection of the polarized signal, for the four MFI frequencies.

– Spectral index in intensity: column `ALPHA_I` gives the colour-corrected spectral index calculated as described in Section 3.6 of Herranz et al. [2023]. Its associated error is given in column `ALPHA_I err`.

– Spectral index in polarization: column `ALPHA_P` gives the colour-corrected spectral index calculated as described in Section 3.6 of Herranz et al. [2023]. Its associated error is given in column `ALPHA_P err`.

– Flag: source candidates with estimated SN$R < 0$ in at least one frequency are flagged with the number 1. For these sources, the corresponding I column has been set to NaN. The corresponding uncertainty is kept as it may be used as an estimate of the upper flux density limit. We do not provide spectral index estimations for these sources, as they are considered as only marginal detections. There are 14 of these sources in the extended catalogue and zero in the main catalogue. The rest of sources are flagged with the value 0.

– Cross-identifications: for those cases where it is possible, we give the name of possible cross-identifications, within a $30'$ search radius around the position of each MFI source candidate, to the following surveys of radio sources:

– `PCCS2 ID`: nearest matched source in the *Planck* Second Catalogue of Compact Sources [Planck Collaboration et al., 2016].

– `PNCT ID`: nearest matched source in the *Planck* Catalogue of Non-Thermal Sources [Planck Collaboration et al., 2018].

– `Other IDs`: for those cases where it is possible, we also give the nearest match, within a 30′ search radius, to the 3C [Bennett and Simth, 1962] and the Parkes-MIT-NRAO [PMN, Wright et al., 1994] surveys of radio sources.

5 QUIJOTE MFI DR1: component separated maps

5.1 Component separation in polarization

This release includes the polarization component separation products obtained using QUIJOTE MFI 11 and 13 GHz channels, as well as WMAP's K and Ka bands and all polarized *Planck* channels[4], filtered with FDEC de la Hoz et al. [2023]. The maps corresponds to the default case in de la Hoz et al. [2023] where the CMB is modeled as a constant in thermodynamic units, and the synchrotron and thermal dust emission are modeled as a power law and a modified blackbody in antenna units respectively.

The component separation products are presented in HEALPix format with RING ordering, with a default value of $N_{\rm side} = 64$, using Galactic coordinates, and smoothed with a Gaussian beam of FWHM= 2°. The component separated maps are given as

```
{fn}_quijote_mfi_cs_pol_{NSIDE}_dr1.fits
```

where `fn` is the name of the parameter (see Table 6), and `NSIDE`= 64.

The FITS files contain a minimal primary header with no data, and a BINTABLE with the estimated value and the standard deviation of each parameter. The number of extensions depends on the parameter:

1. The amplitudes of the sky components (`CMB`, `As`, and `Ad`) contain 4 extensions: the estimated Q and U values[5] and their uncertainties.

2. The spectral parameters (`betas`, `betad`, and `Td`) contain only 2 extensions: their estimated value and uncertainty respectively.

3. `chi2r` has only one extension with the reduced χ^2 estimator of the fit.

The name of each extension is given in Table 6. Figure 7 shows an example of the component separation products.

[4] We used the fourth release also known as NPIPE.

[5] Stokes Q and U parameter maps follow the COSMO convention for polarization angles from HEALPix.

Table 6: Component separation products in polarization.

Parameter	`fn`	Extensions	Units	Data type
CMB	`CMB`	`cmbQ`, `std cmbQ`	μK_{CMB}	Real*4
		`cmbU`, `std cmbU`		
A_s	`As`	`a_sQ`, `std a_sQ`	μK_{RJ}	Real*4
		`a_sU`, `std a_sU`		
A_d	`Ad`	`a_dQ`, `std a_dQ`	μK_{RJ}	Real*4
		`a_dU`, `std a_dU`		
β_s	`betas`	`beta_s`, `std beta_s`	none	Real*4
β_d	`betad`	`beta_d`, `std beta_d`	none	Real*4
T_d	`Td`	`T_d`, `std T_d`	K	Real*4
χ^2_{red}	`chi2r`	`chi2_r`	none	Real*4

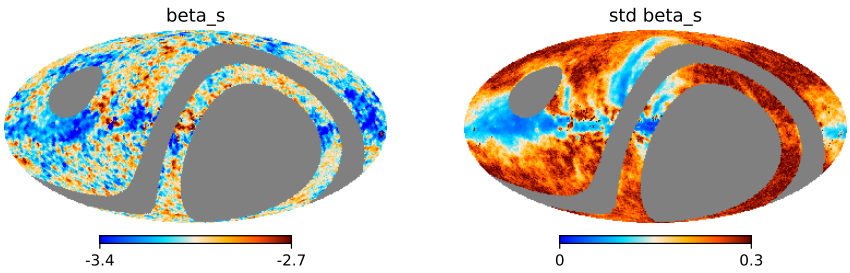

Figure 7: β_s estimate and uncertainty maps.

Parameter	{par}	Extensions	Units	Data type
$I_{1\,\mathrm{GHz}}$	Isyn	Isyn, std_Isyn	MJy/sr	Real*4
α_{syn}	alphasyn	alphasyn, std_alphasyn	none	Real*4
EM	EM	EM, std_EM	pc/cm^6	Real*4
I_{AME}	Iame	Iame, std_Iame	MJy/sr	Real*4
ν_{AME}	nuame	nuame, std_nuame	GHz	Real*4
W_{AME}	Wame	Wame, std_Wame	none	Real*4
τ_{353}	tau353	tau353, std_tau353	none	Real*4
β_{d}	betad	betad, std_betad	none	Real*4
T_{d}	Td	Td, std_Td	K	Real*4
ΔT_{CMB}	DeltaTcmb	DeltaTcmb, std_DeltaTcmb	μK	Real*4

Table 7: Parameter maps included in the release files covering the intensity component separation study in the Galactic plane [Fernández-Torreiro et al., 2023]. Each file contains both the parameter map and its uncertainty map.

Keywords in the extended header indicate the coordinate system ("GALACTIC"), the HEALPix ordering scheme ("RING"), the "COSMO" polarization convention is specified in the "POLCCONV" keyword, and the "BAD_DATA" keyword gives the value used by HEALPix to indicate pixels for which no signal is present. Finally, the "COMMENT" fields provide a summary of the product.

5.2 Component separation in intensity for the Galactic plane

A set of maps describing the microwave sky components (CMB anisotropies and its foregrounds) in intensity along the Galactic Plane ($|b| < 10^\circ$) is also included in this release. Those foregrounds consists of synchrotron, free–free, anomalous microwave emission (AME) and thermal dust components, resulting from the component separation process described in Fernández-Torreiro et al. [2023]. The component maps were produced at 1 degree resolution, and with a HEALPix pixelization of $N_{\mathrm{side}} = 64$. The full set of maps is available in the file

`{par}_quijote_mfi_cs_int_galplane_64_dr1.fits`

where {par} accounts for the different parameters describing the foregrounds. Their actual names are show in Table 7. As in the case of the products described in Section 5.1, the first extension holds a minimal header, while the second extension stores the parameter maps. The structure for this second extension is detailed in Table 7. Each parameter map is accompanied by its standard deviation map. An example for both is shown in Fig. 8. The standard deviation values are computed from the marginalized posteriors from each pixel. These marginalized posteriors can be shared on request, as well as further maps derived from them (e.g. dust radiance, $\mathfrak{R}_{\mathrm{dust}}$, AME emissivity $A_{\mathrm{AME}}/\tau_{353}$, ...).

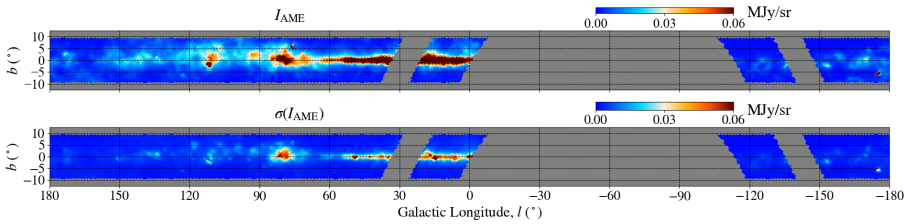

Figure 8: Example of the parameter maps obtained for the Galactic Plane in intensity [Fernández-Torreiro et al., 2023]. We show the AME intensity, $I_{\rm AME}$ (top panel), together with its uncertainty (bottom panel).

Parameter	{par}	Extensions	Units	{Nside}
Zeroth synchrotron moment*	sync_zeroth_moment	Q/U_POLARIZATION	μK_{RJ}	64
β_s modulated synch. amplitude**	sync_first_moment	Q/U_POLARIZATION	μK_{RJ}	64
β_s	betas	BETA_S, STD_BETA_S	None	32
β_s over 21 regions	betas_regions	BETA_S, STD_BETA_S	None	32

* See Eq.12 of Adak et al. [2025]
** This is a derived quantity from zeroth and first order moment maps following Eq.13 of Adak et al. [2025]

Table 8: Description of the maps derived in Adak et al. [2025].

5.3 Component separation with semi-blind technique

This release also includes the reconstructed moment maps of the synchrotron polarisation applying cPILC technique [Adak, 2021], and the derived synchrotron spectral index map by fitting the zeroth and first moments as discussed in Adak et al. [2025]. The moment maps are obtained using data from QUIJOTE 11 and 13 GHz combined maps (with 55 % and 45 % weights respectively), WMAP K and Ka band and *Planck* PR3 LFI data at 30 GHz. These maps are at 22.8 GHz at $N_{\rm side} = 64$ with 2° beam resolution and in μK_{RJ} units. The spectral index maps are derived by fitting the derived moment maps and therefore these maps are at lower resolution of $N_{\rm side} = 32$. The full set of maps is available in RING HEALPix conversion in the filename,

`{par}_quijote_mfi_cpilc_pol_{Nside}_dr1.fits.`

The extensions, {par} and {Nside} are listed in Table 8.

We have also provided the masks at $N_{\rm side} = 64$ used for analysing the 30 % high signal-to-noise region of QUIJOTE-MFI survey. This mask is given in

`GAL_NPS_mask_cpilc_nside64.fits.`

The mask that defines the the 21 patches is given at $N_{\rm side} = 64$ in file name

`region_index_map_cpilc_nside64.fits.`

History

- v1. First version of the document, released on January 12th, 2023.
- v1.1. Updated version, released on May 12th 2023, including the component separated maps in intensity from Fernández-Torreiro et al. [2023] and described in Sect. 5.2.
- v1.1b. Minor update on March 7th 2024, including some clarifications in Sect. 2.4 on the units of the bandpasses.
- v1.2. Released on October 22nd, 2025. Including the moment maps and synchrotron spectral indices using the cPILC method [Adak et al., 2025].

References

J. A. Rubiño-Martín, F. Guidi, R. T. Génova-Santos, S. E. Harper, D. Herranz, R. J. Hoyland, A. N. Lasenby, F. Poidevin, R. Rebolo, B. Ruiz-Granados, F. Vansyngel, P. Vielva, R. A. Watson, E. Artal, M. Ashdown, R. B. Barreiro, J. D. Bilbao-Ahedo, F. J. Casas, B. Casaponsa, R. Cepeda-Arroita, E. de la Hoz, C. Dickinson, R. Fernández-Cobos, M. Fernández-Torreiro, R. González-González, C. Hernández-Monteagudo, M. López-Caniego, C. López-Caraballo, E. Martínez-González, M. W. Peel, A. E. Peláez-Santos, Y. Perrott, L. Piccirillo, N. Razavi-Ghods, P. Scott, D. Titterington, D. Tramonte, and R. Vignaga. QUIJOTE scientific results - IV. A northern sky survey in intensity and polarization at 10-20 GHz with the multifrequency instrument. *MNRAS*, 519(3):3383–3431, March 2023. doi: 10.1093/mnras/stac3439.

D. Herranz, M. López-Caniego, C. H. López-Caraballo, R. T. Génova-Santos, Y. C. Perrott, J. A. Rubiño-Martín, R. Rebolo, E. Artal, M. Ashdown, R. B. Barreiro, F. J. Casas, E. de la Hoz, M. Fernández-Torreiro, F. Guidi, R. J. Hoyland, A. N. Lasenby, E. Martínez-González, M. W. Peel, L. Piccirillo, F. Poidevin, B. Ruiz-Granados, D. Tramonte, F. Vansyngel, P. Vielva, and R. A. Watson. QUIJOTE scientific results - IX. Radio sources in the QUIJOTE-MFI wide survey maps. *MNRAS*, 519(3):3526–3545, March 2023. doi: 10.1093/mnras/stac3657.

E. de la Hoz, R. B. Barreiro, P. Vielva, E. Martínez-González, J. A. Rubiño-Martín, B. Casaponsa, F. Guidi, M. Ashdown, R. T. Génova-Santos, E. Artal, F. J. Casas, R. Fernández-Cobos, M. Fernández-Torreiro, D. Herranz, R. J. Hoyland, A. N. Lasenby, M. López-Caniego, C. H. López-Caraballo, M. W. Peel, L. Piccirillo, F. Poidevin, R. Rebolo, B. Ruiz-Granados, D. Tramonte, F. Vansyngel, and R. A. Watson. QUIJOTE scientific results - VIII. Diffuse polarized foregrounds from component separation with QUIJOTE-MFI. *MNRAS*, 519(3):3504–3525, March 2023. doi: 10.1093/mnras/stac3020.

R. T. Génova-Santos, J. A. Rubiño-Martín, et al. Data proccesing pipeline for the Multi-Frequency Instrument of the *QUIJOTE* experiment. *MNRAS, in prep.*, 2023.

Mike W. Peel, Ricardo Genova-Santos, C. Dickinson, J. P. Leahy, Carlos López-Caraballo, M. Fernández-Torreiro, J. A. Rubiño-Martín, and Locke D. Spencer. Fastcc: Fast Color Corrections for Broadband Radio Telescope Data. *Research Notes of the American Astronomical Society*, 6(12):252, December 2022. doi: 10.3847/2515-5172/aca6eb.

Planck Collaboration, P. A. R. Ade, N. Aghanim, F. Argüeso, M. Arnaud, M. Ashdown, J. Aumont, C. Baccigalupi, A. J. Banday, and R. B. Barreiro. Planck 2015 results. XXVI. The Second Planck Catalogue of Compact Sources. *A&A*, 594:A26, Sep 2016. doi: 10.1051/0004-6361/201526914.

Planck Collaboration, Y. Akrami, F. Argüeso, M. Ashdown, J. Aumont, C. Baccigalupi, M. Ballardini, A. J. Banday, R. B. Barreiro, and N. Bartolo. Planck intermediate results. LIV. The Planck multi-frequency catalogue of non-thermal sources. *A&A*, 619:A94, Nov 2018. doi: 10.1051/0004-6361/201832888.

A. S. Bennett and F. G. Simth. The Preparation of the Revised 3C Catalogue of Radio Sources. *Monthly Notices of the Royal Astronomical Society*, 125 (1):75–86, 07 1962. ISSN 0035-8711. doi: 10.1093/mnras/125.1.75. URL `https://doi.org/10.1093/mnras/125.1.75`.

A. E. Wright, M. R. Griffith, B. F. Burke, and R. D. Ekers. The Parkes-MIT-NRAO (PMN) surveys. 2: Source catalog for the southern survey (delta greater than -87.5 deg and less than -37 deg). *ApJS*, 91:111–308, March 1994. doi: 10.1086/191939.

M. Fernández-Torreiro, J. A. Rubiño-Martín, C. H. López-Caraballo, R. T. Génova-Santos, M. W. Peel, F. Guidi, S. E. Harper, E. Artal, M. Ashdown, R. B. Barreiro, F. J. Casas, E. de la Hoz, D. Herranz, R. Hoyland, A. Lasenby, E. Martínez-Gonzalez, L. Piccirillo, F. Poidevin, R. Rebolo, B. Ruiz-Granados, D. Tramonte, F. Vansyngel, P. Vielva, and R. A. Watson. QUIJOTE scientific results - X. Spatial variations of Anomalous Microwave Emission along the Galactic plane. *MNRAS*, 526(1):1343–1366, November 2023. doi: 10.1093/mnras/stad2545.

Debabrata Adak. A new approach of estimating the galactic thermal dust and synchrotron polarized emission template in the microwave bands. *Monthly Notices of the Royal Astronomical Society*, 507(3):4618–4637, 08 2021. ISSN 0035-8711. doi: 10.1093/mnras/stab2392. URL `https://doi.org/10.1093/mnras/stab2392`.

Debabrata Adak, J. A. Rubiño-Martín, R. T. Génova-Santos, M. Remazeilles, A. Almeida, K. Aryan, M. Ashdown, R. B. Barreiro, U. Bose,

R. Cepeda-Arroita, J. M. Casas, M. Fernández-Torreiro, E. Martínez-Gonzalez, F. Poidevin, R. Rebolo, and P. Vielva. QUIJOTE scientific results XIX. New constraints on the synchrotron spectral index using a semi-blind component separation method. *arXiv e-prints*, art. arXiv:2510.17761, October 2025.